

# A prognosis case study for electrolytic capacitor degradation in DC-DC converters

Chetan S. Kulkarni<sup>1</sup>, Gautam Biswas<sup>1</sup>, and Xenofon Koutsoukos<sup>1</sup>

<sup>1</sup> *Institute for Software Integrated Systems  
Department of Electrical Engineering and Computer Science  
Vanderbilt University, Nashville, TN 37235  
chetan.kulkarni, gautam.biswas, xenofon.koutsouko@vanderbilt.edu*

## ABSTRACT

This paper proposes a model based approach for prognosis of DC-DC power converters. We briefly review the prognosis process, and present an overview of different approaches that have been developed. We study the effects of capacitor degradation on DC-DC converter performance by developing a combination of a thermal model for ripple current effects and a physics of failure model of the thermal effects on capacitor degradation. The derived degradation model of the capacitor is reintroduced into the DC-DC converter model to study changes in the system performance using Monte Carlo methods. The simulation results observed under different conditions and experimental setups for model verification are discussed. The paper concludes with comments and future work to be done.

## 1 INTRODUCTION

Prognostics and health management (PHM) methodologies evaluate reliability of a system under actual life-cycle conditions (Kalgren and et al, 2007). In particular ‘prognostics’ covers the process of predicting future system states based on the current conditions and past operations. Overall PHM is directed towards achieving multiple practical goals, such as systems safety, reductions in operational and support (O&S) costs, maintenance costs, and the life cycle total ownership costs (TOC) (Pecht *et al.*, 2007). For safety critical systems, which require constant monitoring of the systems and its components, prognosis methods can play a very important role in predicting the evolving conditions of the components. This helps make important replacement decisions as components reach the safe limits of their useful life cycle. Diagnostic monitoring systems assist the predictive process

This is an open-access article distributed under the terms of the Creative Commons Attribution 3.0 United States License, which permits unrestricted use, distribution, and reproduction in any medium, provided the original author and source are credited.

by providing the initial detection and isolation capabilities (Kalgren and et al, 2007; Pecht *et al.*, 2007).

Our project focuses on developing and implementing effective diagnostic and prognostic technologies with the ability to detect faults in the early stages of degradation. Early detection and analysis may lead to better prediction and end of life estimates by tracking and modeling the degradation process. The idea is to use these estimates to make accurate and precise prediction of the time to failure of components. Early detection also helps in avoiding catastrophic failures.

We adopt a model based approach based on physical bond graph models of the system to predict the dynamic behavior of the system under nominal and degraded conditions (Karnopp and Rosenberg, 1983). Faults and degradations appear as parameter value changes in the model, and this provides the mechanisms for tracking system behavior under degraded conditions. In this paper, we apply our model based prognostics methodology to the DC-DC power supplies that are used in many electronic systems. In these systems, electrolytic capacitors and MOSFET switches are known to have the highest degradation and failure rates among all of the components (Goodman and et al, 2005). Degraded capacitors affect the performance and efficiency of the DC-DC converters in a significant way. The paper develops a method for studying the degradation effects of electrolytic capacitors subject to ripple currents, and their impact on overall system performance.

The paper is organized as follows. Section II presents a high level overview of the different prognostics methods reported in the literature. Section III describes in detail the DC-DC converter model. In section IV we discuss our approach for building a physics based electrolytic capacitor degradation model. Simulation studies on the converter model are discussed in section V. The section also discusses proposed experimental setups for correcting model parameters and verification. The paper concludes with discussion of the experimental results and future work.

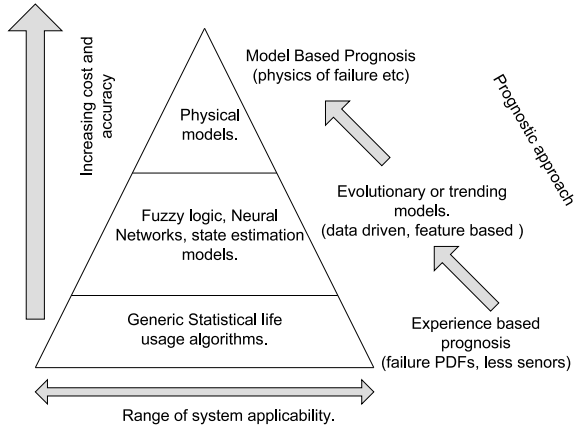


Figure 1: Prognosis Technical Approaches.

## 2 PROGNOSTICS METHODS

A number of different methods have been applied to study prognosis of degraded components. In general, prognostics approaches can be classified into three primary categories: (1) model driven, (2) data driven and (3) probability based prognostic techniques. Fig. 1 summarizes the range of prognosis approaches applied to different systems and their relative cost for implementation and operation.

Model based prognostic techniques use dynamic models of the process for predicting degradation behavior. These approaches apply to situations where accurate mathematical models of system behavior can be constructed from first principles. Residuals that capture the difference between the measurements of a real system and the outputs of the mathematical models are used to detect and isolate degradations in the system. Statistical techniques ensure robustness in the detection task. Isolation and identification are achieved by methods, such as parity relations, observers, and parameter estimation (Vachtsevanos, 2006). Model-based methods in conjunction with empirical physics of failure models provide mechanisms for calculating the damage and degradation in critical components of the system as a function of the operating conditions and the present condition (Vachtsevanos, 2006). However, developing complete and accurate state space models of the degradation process in a complex system may be practically infeasible.

Statistical models of historical operational profiles, represented as standard probability density functions (pdf), provide an alternate methodology for calculating future damage accumulation. The results from such models can be used for real-time failure prognostic predictions with confidence bounds.

In contrast to model-based and statistical approaches, data-driven techniques primarily rely on process health data to model a relationship between the data features and different fault classes. Thus, in data driven techniques probability distributions are derived depending upon the amount of available data. The data is monitored using specific sensors that are tailored to capture faulty behavior that is linked to the system requirements. In many applications, measured

input/output data are often the only source for studying and understanding system degradation behavior. Data-driven approaches rely on the assumption that the statistical characteristics of data are relatively unchanged till a malfunctioning event occurs in the system (Luo *et al.*, 2003).

Many data-driven approaches use statistical learning techniques derived from pattern recognition and machine learning theories (Luo *et al.*, 2003). These include probabilistic neural networks (PNN), dynamic wavelet neural networks (DWNN), graphical Bayesian network models, hidden Markov models, self-organizing feature maps, signal analysis filters, auto-regressive models, FFT, and fuzzy rule-based systems. Typically data driven approaches have higher accuracy and cost as compared to the probability based techniques, but they may be more cost effective and less accurate as compared to model driven approaches (Schwabacher, 2005). When additional sensors need to be added to gather more data, data driven techniques can become expensive, especially for legacy systems.

Combined statistical and data driven methods that rely on historical data of previous failures in the given system is another approach that is often applied for prognostic analysis. Starting with the assumption that the statistical distribution of the degradations are known, the data may be used to derive the parameters of the known pdf function. If no assumptions are made about the degradation distribution, the data may be employed to derive an empirical distribution. These combined methods are often more effective because they require less detailed information than differential equations of the model-based techniques. The pdfs of the captured data typically are sufficient to predict required parameters of interest for prognosis. Statistical methods also provide confidence limits, which are important for confirming the accuracy and precision of the predictions. An example of probabilistic approaches used for degradation modeling include the Weibull distribution models.

Earlier work for DC-DC converters was mainly done for reliability of the complete system. Model based as well as data driven approaches have been used for verifying the converter model for its reliability and working (Delgado and Sira-Ramrez, 1998; Vorperian., 1990). Previous prognosis work does not discuss component level degradation and their effects on the system efficiency. Our approach in this paper combines model based and stochastic approaches for predicting degradations and future system behavior under degraded conditions. We use systematic methods to develop physical models of the DC-DC converter, and a combination of physical and physics of failure models to represent capacitor degradation. Stochastic Monte Carlo approaches are then employed to study the effect of capacitor degradation on converter output.

## 3 DC-DC CONVERTERS

Switched-mode power supplies are widely used in DC-DC converters because of their high efficiency and compact size. DC-DC converters are important in portable electronic devices, which derive their power

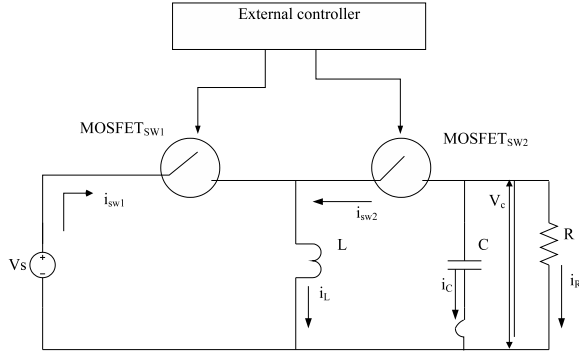


Figure 2: Buck Boost Converter Circuit

primarily from batteries. Such electronic devices often contain several sub-circuits with different voltage requirements (sometimes higher and sometimes lower than the supply voltage, and possibly even negative voltage). DC-DC converters can provide additional functionality for boosting the battery voltage as the battery charge declines.

A typical buck-boost DC-DC converter circuit is illustrated in Fig. 2. Such converters convert from one voltage level to another, by storing the input energy temporarily in inductors when switch sw1 is ON and switch sw2 is OFF, and then releasing that energy to the output at a different voltage value when sw2 is ON and sw1 is turned OFF. The efficiency of conversion ranges from 75% to 98%. This high efficiency is typically achieved by using power MOSFET's (metal oxide semiconductor field-effect transistor), which can provide high frequency switching more efficiently than power bipolar transistors, which, in addition to greater switching losses require more complex drive circuits. Overall, MOSFET switches increases the battery life in such devices. A buck boost approach is used for conversion to the required dc voltage output. Our particular application has an input of 28V DC from a battery source, and the required output voltage is 5V. The switches sw1 and sw2 are power MOSFET's, which are controlled by an external controller. Fig. 2 shows the external controller box, which controls the switching of the MOSFET's to maintain the required output voltage. We use the Bond Graph modeling approach (Karnopp and Rosenberg, 1983) for modeling the DC-DC converter.

Our proposed approach is to develop a systematic approach for reliable diagnostics and prognostics for the converter system. For this we need to capture the topological and functional dependence of the system in addition to component level faults and capturing the causal flow in time to account for transient failures.

The primary objective in this work is to develop a modeling framework that captures these features. There are two elements to this framework. The first is capturing and implementing the system model and physics of failure models at the component level. The second element is embedding this knowledge in a topological modeling language called Bond Graphs (BG), which provide a framework for building systematic, energy-based component models of the system,

Table 1: Basic Bond graph elements.

Symbol	Type of element	Name of element	Electric domain
C	storage	capacitance	capacitor
L		inductance	inductor
R	dissipator	resistance	resistor
TF	transducer	transformer	transformer
GY		gyrator	
Se	source	effort source	voltage source
Sf		flow source	current source
1	junction	1-junction	serial connection
0		0-junction	parallel connection

which can then be easily composed to define system-level models. A detail description of the bond graph models for the DC-DC converter and capacitor are discussed in the next section.

### 3.1 Bond Graph Modeling

Model-based identification methodologies require system models that accurately represent system dynamics and are also capable of linking system measurements to damage in the components of the model. The bond graph modeling framework provides both these features (Karnopp and Rosenberg, 1983). Bond graphs provide a systematic framework for lumped parameter modeling across multiple domains that include the electrical, mechanical, hydraulic, and thermal domains (Gawthrop and Smith, 1996; Dragan Antic and Mladenovic, 1999). Bond graphs (BGs) are an explicit topological modeling language for capturing the dynamic energy transfer among components of a systems based on the principles of continuity of power and conservation of energy.

This energy distribution reflects the history of the system and, therefore, defines its state at a point in time. Behavior of the system at future time points is determined by the current state description and subsequent input to the system (Dragan Antic and Mladenovic, 1999). Changes in the state of the physical system are attributed to energy exchange among its components, which can be expressed in terms of power (time derivative of flow of energy). A fundamental principle of bond graphs is that power transmitted between connected components can be expressed as a product of 'effort' and 'flow', irrespective of the domain in which they are implemented (Gawthrop and Smith, 1996).

Bond graph elements are classified into one of five basic elements, (1) energy storage elements, Capacitance (C), the Inertia (I), (2) the dissipative element, Resistor (R), (3) two idealized energy transformation elements, the transformer (TF) and the Gyrator (GY), (4) two source elements,  $S_e$ , source of effort and  $S_f$ , source of flow, and (5) two junction ele-

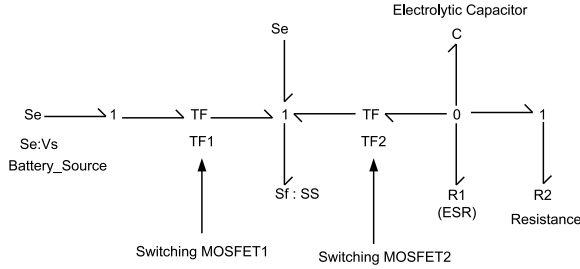


Figure 3: Buck Boost Converter Bond Graph Model

ments, 0 (for parallel connections) and 1 (for series connections). All these elements exchange energy with other elements through ports or bonds. Bonds are energy transfer pathways that connect elements and junctions and are represented as half arrows. Effort and flow signals are the information transferred through these pathways (Gawthrop and Smith, 1996; Dragan Antic and Mladenovic, 1999).

The two ideal source elements model energy flow in and out of a system. These two elements are active elements since they introduce energy into the system. All the other elements are passive (Dragan Antic and Mladenovic, 1999).

### 3.2 DC-DC converter model

A passivity based approach discussed in (Garcia-Gomez *et al.*, 2006) is used for deriving the BG model of the buck boost converter. This approach models the system behavior in two stages: (i) an energy shaping stage, where the closed loop total energy of the system is modified, and (ii) a damping injection stage, where the required dissipation is added in order to achieve asymptotic stability (Garcia-Gomez *et al.*, 2006).

The bond graph of the passivity based buck boost converter model is shown in Fig. 3.  $Se:Vs$  is the battery voltage. The switching elements  $sw1$  and  $sw2$  are replaced by modulating transformers (MTFs).

The representation of the switching devices as MTFs is derived directly from the algebraic relations of the effort and flow variables. In an average model of the buck-boost converter, the switching bond is replaced by a 'duty-ratio-modulated bond'. This 'average' bond can be effectively interpreted as an ideal lossless transformer with turns ratio specified by the complementary duty ratio function associated with the controlling scheme. The switching frequency of the the MTFs depend upon the value  $\alpha$ . The value of  $\alpha$  is calculated from the values of  $R_2$ ,  $C$ ,  $L$  and the input/output voltage requirements. (Garcia-Gomez *et al.*, 2006) provides the detailed equations used for deriving the value of  $\alpha$ .

The regulation of the converter output at a desired output voltage  $v_{Cd}$  depends on the steady state value of the average inductor current  $i_L$ . This is determined by replacing dynamic element  $L$  (inductor) of the average bond graph by a SS-element (source-sensor element), represented as flow source  $Sf$  in the BG. The desired steady state value for the current can then be obtained as  $i_L = (1 + v_{Cd}/v_s)v_{Cd}/R_2$ . An input injection from the external passivity controller to the modulated effort source is added to the bond graph model of DC-DC

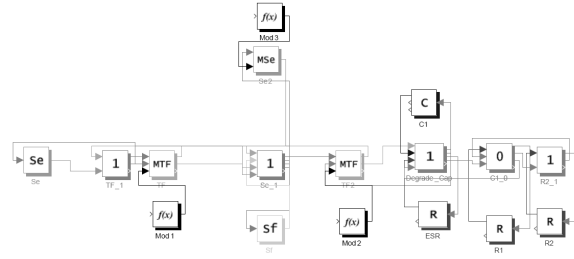


Figure 4: Buck Boost Converter Simulink Model

converter in the form of a  $Se$  element. (Garcia-Gomez *et al.*, 2006) provides more details.

For conversion of the topological bond graph model to its equivalent MATLAB/ SIMULINK<sup>®</sup> model we use the approach presented in (Roychoudhury *et al.*, 2008). An interpreter is used for converting the BG model into an intermittent block diagram model from which the simulation model is derived. In its first stage, the interpreter navigates through the model hierarchy, mapping all the BG elements to block diagram (BD) elements. The second stage of the interpretation process consists of generating the simulation components from the BD model. The BD has all the required information for generating the simulation model. The generated simulation model from the BG model is shown in Fig. 4. Once the MATLAB/ SIMULINK<sup>®</sup> model is generated, the required simulation results can be observed under different operating conditions. These are explained in a later section of the paper. Our approach in the paper is to develop physics of failure models of degrading capacitors, and use them to simulate the degradation behavior of DC-DC converters.

### 3.3 Component Degradation/Failure

It has been reported in the literature that the capacitors and transistors degrade faster than any other components in the DC-DC converters (Imam *et al.*, 2005). Degradation in these components leads to decrease in the operating efficiency of the converters and eventually failure in the system.

Electrolytic capacitors are the leading cause for breakdowns in power supply systems. The performance of the electrolytic capacitor is strongly affected by its operating conditions, which includes voltage, current, frequency, and working temperature. A degraded electrolytic capacitor cannot provide a low impedance path for the ac current in the output filter of these converters, thus introducing a ripple voltage on top of the desired DC voltage. The filter also results in a decrease in the power supply efficiency. Continued degradation of the capacitor will cause the converter output voltage to drop below specifications, and in some cases it may even damage the converter itself.

Power transistor / MOSFET faults are the second leading cause of DC-DC converter failures. Most applications require that the MOSFETs be switched at high frequency. The thermal and electrical changes, the device undergoes during switching is large during the turn-off of the device, and the cause for most of the damage in the MOSFETs.

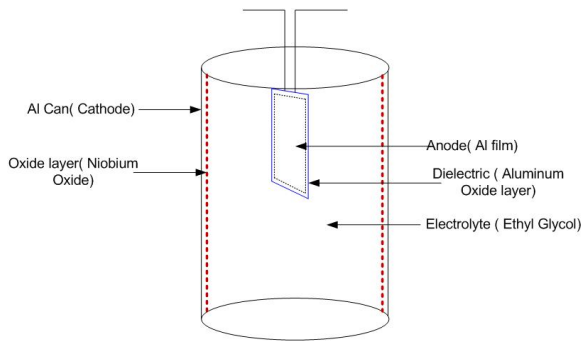


Figure 5: Physical Model of Electrolytic Capacitor.

It is commonly assumed that any mechanism that permits the ‘parasitic’ bipolar transistor to become active will usually lead to failure of the power MOS-FET, particularly if the drain voltage is greater than the collector-emitter sustaining voltage of the ‘parasitic’ bipolar transistor. It has also been observed that avalanche injection in the drain region of the MOS-FET may lead to failure without the parasitic bipolar transistor becoming active.

For this paper we focus on capacitor degradation and their overall effect on the DC-DC converter performance. The detailed analysis for prognosis is carried out in several steps. These are outlined in the next section.

#### 4 ELECTROLYTIC CAPACITOR DEGRADATION MODELS

This section discusses in detail the conditions under which the capacitor degrades leading to faults in the system. We study the adverse effects of ripple currents, which cause degradation by raising the core temperatures in the capacitor core.

##### 4.1 Physical Model of the Capacitor

An aluminum electrolytic capacitor, illustrated in Fig. 5 consists of a cathode aluminum foil, electrolytic paper, electrolyte, and an aluminum oxide layer on the anode foil surface, which acts as the dielectric. When in contact with the electrolyte, the oxide layer possesses an excellent forward direction insulation property. Together with magnified effective surface area attained by etching the foil, a high capacitance is obtained in a small volume (Fife, 2006).

Since the oxide layer has rectifying properties, a capacitor has polarity. If both the anode and cathode foils have an oxide layer, the capacitors would be bipolar type capacitor. In this paper we analyze ‘non-solid’ aluminum electrolytic capacitors in which the electrolytic paper is impregnated with liquid electrolyte. There is another type of aluminum electrolytic capacitor, that uses solid electrolyte but we will not referring to these types in this work (Fife, 2006; Bengt, 1995).

##### 4.2 Degradation Mechanisms

There are several factors that cause degradation in electrolytic capacitors. The degradation over a period of time finally results in the failure of the component, which impacts the working of the subsystems that are part of the system. The definition of failure and some of the failure modes are discussed below.

Failures in a capacitor can be one of two types: (1) catastrophic failures, where there is complete loss of functionality due to a short or open circuit and (2) degradation failures, where there is gradual deterioration of capacitor function. Degradation failures manifest as an increase in the equivalent series resistance (ESR) and decrease in capacitance over time. Continued degradation over time leads to failure of the component.

Capacitor degradation is typically attributed to :

1. High Voltage conditions: The capacitance decreases and ESR increases.
2. Transients : The leakage current can be high and an internal short-circuit can occur.
3. Reverse Bias : The leakage current becomes high with loss of capacitance and increase in ESR.
4. Strong Vibrations : These can cause internal short circuits, capacitance losses, high leakage currents, high ESR and open circuits.
5. High Ripple current : These cause internal heating ,increasing the core temperature which results in gradual aging of the capacitor.

As stated earlier, our focus in this work is on degradation effects in the capacitor caused by ripple currents generated in the DC-DC converter. We will be working on the other causes of capacitor degradation and develop those models using the BG approach. These models will be then combined to study the over effect of degradation of capacitors due to these factors. Ripple current refers to the AC portion of the current signal applied to a device. Although this term defines an AC portion of the applied signal, it is more generally attributed to the small level of variation of DC signals encountered in a power supply system.

The wearout of aluminum electrolytic capacitors is due to vaporization of electrolyte that leads to a drift in the main electrical parameters of the capacitor. One of the primary parameters is the equivalent series resistance (ESR). The ESR of the capacitor is the sum of the resistance due to aluminum oxide, electrolyte, spacer, and electrodes (foil, tabbing, leads, and ohmic contacts). The health of the capacitor is often measured by the ESR value. Over the operating period, the capacitor degrades i.e its capacitance decreases and ESR increases. Depending upon the percentage increase in the ESR values we can evaluate the healthiness of the capacitor. Considering the current ESR value and operating conditions the remaining useful life of the capacitor can be calculated using model based methods. There are certain industry standards for these parameter values, if the measurements exceed these standards then the component is considered failed i.e. it has reached its end of life, and should be immediately replaced before further operations.

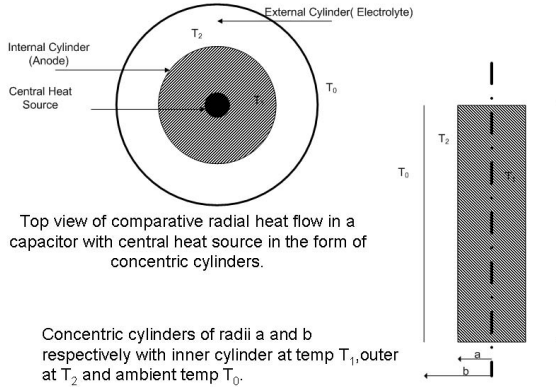


Figure 6: Comparative Radial Heat Flow in Electrolytic Capacitor

Ripple currents produce additional heat inside a capacitor (Chen, 2004). As the internal temperature increases the electrolyte evaporates. The decrease in electrolyte affects both the capacitance value and the ESR, which in turn can cause increases in the output ripple current, thus causing a vicious cycle, and faster capacitor degradation. We plan to study this phenomena in greater detail in the future.

A first step in calculating the increase in ESR due to ripple current involves determining the internal core temperature in the capacitor. This requires the construction of a thermal flow model that captures the heat dissipation from the core to the ambient surroundings of the capacitor.

### 4.3 Thermal Model

The maximum permissible ripple current in a capacitor depends on factors, such as the capacity of the leads, lugs and terminals to withstand maximum current. However, the most important factor is the raised temperature in the capacitor core, which causes the electrolyte to evaporate (R.P.Tye, 1968). It has been observed that the temperature of the cartridge remains almost constant across the diameter and along the length of the capacitor. This is also true for the casing. Therefore, it is reasonable to assume that cartridge and casing are isothermal bodies. As a result, the capacitor can be treated as two concentric isothermal cylinders as shown in Fig. 6 with temperature values  $T_1$  and  $T_2$ , respectively. Further heat flow can be considered to be radial. These assumptions hold for capacitors having cylindrical surface area much greater than the end areas (Gasperi, 1996).

Heat generation in the capacitor takes place at the core, from where it travels radially outwards towards the surface as explained earlier. The heat generation can be attributed to the ripple current passing through the ESR of the capacitor. The capacitor thermal model is shown in Fig. 7. Here the heat flow is considered only in one direction from the core to the outer surface. The capacitor structure is made up of different layers through which the heat flow occurs before it is radiated out to the surrounding atmosphere. In the thermal model these layers represent successive thermal capacitances and thermal resistances. In the capacitor,

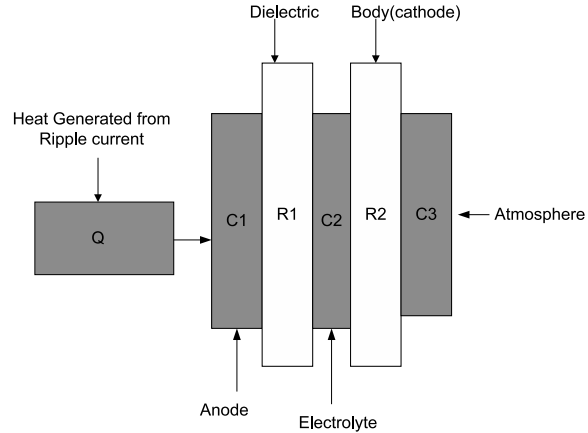


Figure 7: Thermal Model of Electrolytic Capacitor

the anode and electrolyte layers along with the ambient surrounding are represented as the thermal capacitances, labeled as  $C_1$ ,  $C_2$  and  $C_3$ , respectively. This is shown in the Fig. 7. Similarly the dielectric and body (cathode) layers are modeled as thermal resistances  $R_1$  and  $R_2$ , respectively.

A bond graph modeling approach is used to model the heat transfer from the capacitor core to the ambient surroundings, and use this model to establish the steady state temperature of the capacitor core. The details of the model are discussed below.

### Capacitor Bond Graph model

A complete BG model derived from the thermal model is shown in the Fig. 8. The thermal capacitance  $C_3$  of the ambient surrounding is calculated considering a small open space around the capacitor capsule. This small space around the capacitor capsule is assumed to be constant, hence conduction type of heat transfer between the capsule and surrounding is considered instead of convection type of heat transfer. A small thermal resistance value, denoted by  $R$ , which dissipates heat to the surrounding atmosphere is considered. The calculations of the capacitor and resistance values are a function of the capacitor dimensions and the materials used. The amount of heat generated  $Q$  is given by  $I_{rms}^2 \times ESR$ , where  $I_{rms}$  is the rms (root mean square) value of the ripple current (in amperes), and ESR (in ohms). The heat is generated at the core of the capacitor cartridge, i.e., at the anode.

The next section discusses in detail the physics of failure models used to represent the degradation process in electrolytic capacitors.

### 4.4 Physics of Failure Models for Capacitor Degradation

Life prediction (Lahyani *et al.*, 1998) and Failure prediction (Chen, 2005) are the two methods used to model electrolytic capacitor degradation. Depending upon the value of ESR, the remaining useful life (RUL) of the capacitor can be predicted for a given operating period under specific operating conditions. In the Life prediction method, ESR is calculated considering the increase in the temperature due to the ripple current,

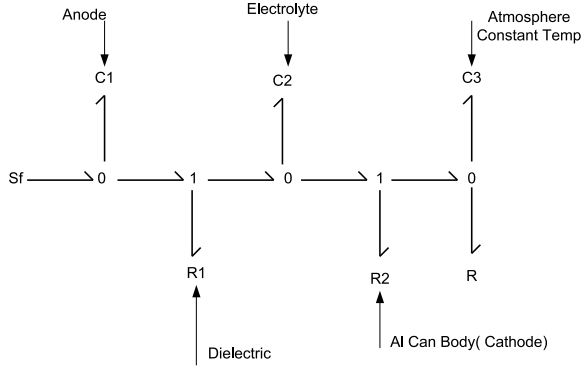


Figure 8: Bond Graph Model of Electrolytic Capacitor

while in Failure prediction method the ESR is calculated from the variations in output voltage and current of the DC-DC converter. In this work we focus on the Life prediction method to study the effects on ripple current on capacitor degradation.

**Life Prediction Method**

Typically, thermal degradation affects both the capacitance and ESR values of electrolytic capacitors. (Lahyani *et al.*, 1998; Chen, 2005) report on the change in ESR values due to thermal degradation. A linear inverse model (P. Venet and Grellet, 1993) has been derived as an extension of Arrhenius Law to define the change in ESR value over time for a capacitor subjected to a constant high temperature. The linear inverse model for computing ESR value at time ‘t’ for a given temperature T is given by:

$$\frac{1}{ESR_t} = \frac{1}{ESR_0} (1 - k.t.exp(\frac{-4700}{T + 273})) \quad (1)$$

where :

- $ESR_t$  = the ESR value at time ‘t’.
- T = the temperature at which the capacitor operates.
- t = the operating time.
- $ESR_0$  = initial ESR value at t = 0.
- k = constant which depends on the design and the construction of the capacitor.

The factor k depends on the parameters, such as the size of the capacitor. The value of k is typically determined empirically for a particular class of capacitors. For the simulation study below, we use k values reported in the literature, but we will conduct experiments to determine the value of k in future work.

**4.5 Implementation of Degraded Model in SIMULINK®**

Like before, we derive the MATLAB/ SIMULINK® model of thermal degradation for the electrolytic capacitor from the BG model. The derived MATLAB/ SIMULINK® model is shown in Fig. 9. This model can be used for observing the behavior of the capacitor

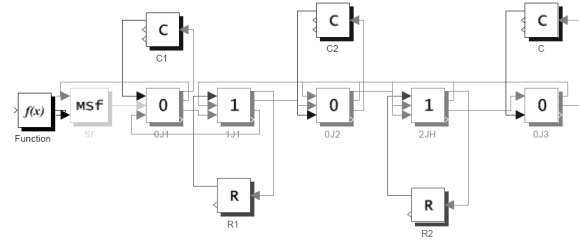


Figure 9: Simulink Model of Electrolytic Capacitor

Table 2: Thermal values of the elements for Capacitor Model.

Thermal Element	Thermal Layer	Thermal Value
C1	Anode	$0.024 \frac{J}{kgK}$
C2	Electrolyte	$3.45 \frac{J}{kgK}$
C	Atmosphere	$0.151 \frac{J}{kgK}$
R1	Dielectric	$0.2 \frac{K}{W}$
R2	Cathode(Body)	$0.16 \frac{K}{W}$

under different experimental and ambient conditions. In the MATLAB/ SIMULINK® model the electrolytic capacitor is simulated for ripple current ( $I_{rms}$ ) values. Experiments are conducted for different values of ambient temperature: (1) 20°C, (2) 45°C and (3) 65°C. The results indicate how the capacitor will behave under these operating conditions.

**5 STUDYING DC-DC CONVERTER DEGRADATION**

To study the effect of degradation of electrolytic capacitors on the DC-DC converters we perform Monte Carlo simulations on the MATLAB/ SIMULINK® model. This is done in two steps. First, we use the capacitor thermal degradation model to study the effects of ripple current on the increase in capacitor core temperature, and use this temperature value to establish how the ESR of the capacitor changes with time. Step 2 considers the effects of the capacitor degradation on the DC-DC converter output. This section discusses the results observed from these simulations.

**Capacitor Model simulation**

For the simulation experiments we calculated the values of the thermal resistances and capacitances using values for standard capacitors that were reported in the literature (Bengt, 1995). Table 2 shows the values for all the elements in the model.

For calculating the amount of heat generated, an initial ESR value of 51mΩ and a maximum current of 1A flowing through the system was considered. The ripple current magnitude was determined relative to the maximum current rating. The increase in temperature is observed for ripple current values of 10, 15 and 20 percent. We simulated the model with ambient temperature values of 20°C , 45°C and 65°C . Gaussian white noise was added to the ripple current and the

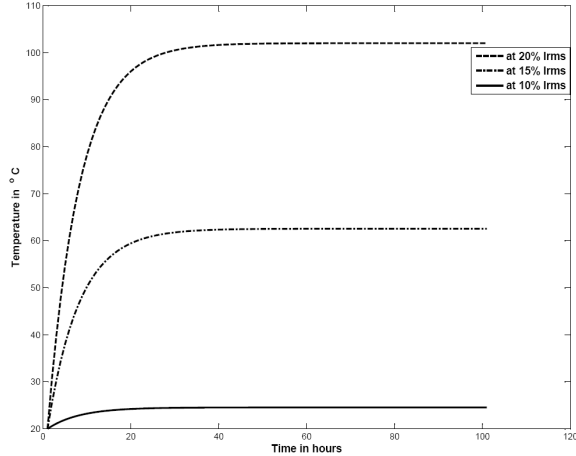


Figure 10: Simulation Output for Temperature at Different Values of Irms Ripple Current

Table 3: Parameter values of the elements for Buck-Boost Model.

Element	Name	Value
R1	ESR	51 m $\Omega$
R2	Resistance	30 $\Omega$
C	Electrolytic Capacitor	200 $\mu$ F
Se	Input Voltage	28 V

variance was chosen to be 5% of the ripple current value. The ambient temperature was kept at a constant value. Fig. 10 shows the results observed for the simulation of the electrolytic capacitor model under the different ripple current values for ambient temperature equal to 20°C. As the ripple current increases the core temperature rises significantly above the normal working temperature.

Over the period of time this affects the working of the capacitors. The increase in the steady state value of the internal temperature causes the electrolyte volume to decrease (by evaporation). This increases the ESR and decreases the capacitance of the capacitor.

### DC-DC converter Model simulation

As a first step we simulated nominal behavior for the buck-boost converter using the parameters listed in Table 3. The input voltage was set at 28V (source battery) and the required DC-DC converter output voltage is given as 5V.

To simulate the effect of capacitor degradation we replaced the nominal capacitor model by the degraded capacitor model. We could not find a model that expressed decrease in capacitance value for a given temperature value. In future studies, we will determine this empirically. For this study, we assumed the capacitor value degrades linearly with time. The coefficient of the linear function depends on the capacitor core temperature. For the ESR the empirical formula of Life prediction method was substituted as a function for ESR degradation. Uncertainties in the model parameters were represented by a Gaussian white noise model, and the sigma value was chosen to be 5% of

Table 4: Degradation effect on Output Voltage

Temperature	Time (hours)	Decrease in Voltage	Increase in ESR
100°C	300	0.19%	0.5%
135°C	300	0.25%	4.3%

the current value for the parameter. In other words, sigma increases as the absolute value of a parameter increases. Therefore, uncertainty in the parameter value increased with time. We used Monte Carlo methods to derive the behavior of the DC-DC converter.

The degradation functions were introduced in the system after the output voltage of the DC-DC converter was stabilized after a certain time of operation. Monte Carlo simulations were carried out for (1) 100°C and (2) 135°C rise in the core temperature. 100°C rise in core temperature is at 20% ripple current and ambient temperature of 20°C, while 135°C rise in core temperature is at 20% ripple current and ambient temperature of 45°C. To study the DC-DC converter performance, the simulation was run for about 300 hours, and the degradation in converter output voltage was plotted as shown in Figure 11. The figure also shows an expanded view of the output voltage, where the variation in the form of ripples in the output voltage can be observed for the two different temperature values. As expected, the voltage output of degraded converter gradually drops as time progresses. At the end of 300 hours, the average output voltage dropped by 0.19% and 0.25% below the nominal 5V value for core temperature values of 100°C and 135°C respectively. The percentage increase in the ESR value for these two temperature values at 300 hours of operation time was calculated as 0.5% and 4.3%, respectively. Table 4 shows the degradation effect on the decrease in the output voltage of the DC-DC converter. In this experiment we have simulated a short working span of capacitor life under certain condition. Thus using the model we can simulate the behaviour of the system under different conditions and help in the prognosis of the converter. For this work we have considered the effect of only electrolytic capacitors on the converters, including models for MOSFETs as discussed in the previous sections will help in predicting the working of the system more effectively.

An increase in the ESR value will cause excessive output ripple voltage and current. As the ESR value increases these overshoots/ripples increase thus increasing the internal working temperature of the capacitor. The increase in the core temperature is responsible for degrading the capacitor over the period of time. Increase in the ripple voltage is a cause of concern to the different devices to which the power supply is connected. The percentage variation in the output voltage depends on the application and sensitivity of the device connected to the DC-DC converter. In some cases a large variation is acceptable while in case of sensitive devices a small variation can affect the working of the device. According to industry standards, an electrolytic capacitor is replaced when its ESR values exceeds 2.8 times its initial value. In systems, where the requirements for output voltages are very stringent, if



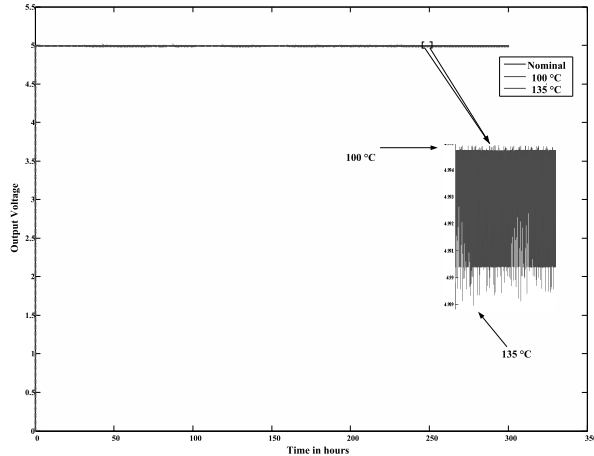


Figure 11: Difference in Nominal and Degraded Capacitor Outputs

the voltage drops below a certain defined percentage value, the capacitor may be replaced. To verify our model we are conducting experiments on electrolytic capacitors which are discussed in the next section.

### Capacitor Degradation Experiments

To verify and compare our model results we are conducting experiments on capacitor degradation. At present we have two different setups for simulating the degradation phenomenon in the capacitors. The setups and the experimental procedure is discussed as below.

1. A batch of capacitors is considered for the experiments.
2. Initial detail measurements for each capacitor for ESR, capacitance is done under room conditions and recorded.
3. The capacitors are subjected to tests under two different setups and working conditions.
4. In the first setup the capacitors are put under electrical and thermal stress. Only the capacitor under test is subject to thermal stress while the rest of the system is working under normal conditions.
5. The measurement for output ripple voltage and current, capacitor capsule temperature is recorded every 8 hours.
6. In the second setup the capacitor is subjected to constant charging/discharging cycle with a fixed resistive load.
7. The charging/discharging cycle is fixed upon the capacitor value and the load. The measurements are recorded at specific intervals.

The schematic diagram of the first setup is shown in the Figure 12. These experiments are presently been conducted under different conditions and setups. Once we get the results from these experiments we will be able to compare them with our model and also with results inputs we can modify the parameters values for efficient models.

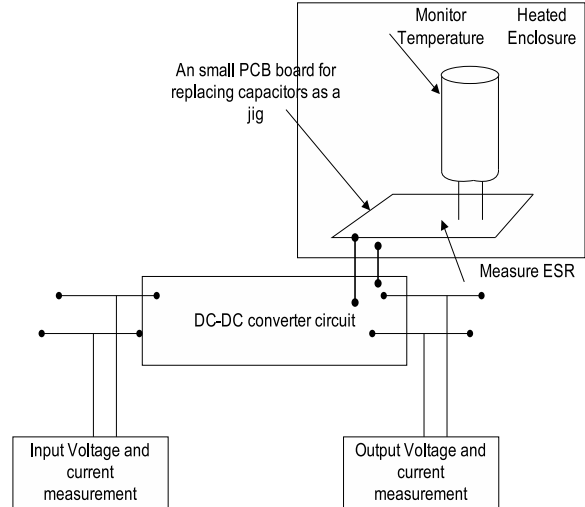


Figure 12: Setup 1 for Electrolytic Capacitor Degradation

## 6 CONCLUSION AND FUTURE WORK

This paper proposes a model-based approach to study electrolytic capacitor degradation in DC-DC converters. The physics of failure model is derived for degradations caused by high ripple currents. The physics of failure model derived expressed the change in ESR and capacitance values as a function of time for given ripple current values and ambient temperature.

It is seen from the simulation results for the capacitor degradation model, that with the increase in the ripple current the core temperature increased significantly. These results were then implemented in the Life prediction model for capacitor degradation in the DC-DC converter models. The simulation observations for DC-DC converter under degraded conditions showed that there was decrease in the output voltage value with an increase in the ESR value over given operation time.

Future work includes conducting laboratory experiments on the electrolytic capacitors. One of the important outputs of these experiments will be comparison of the simulation results with the actual laboratory experimental data. The comparison will provide a methodology for more accurate estimation of model parameters, and, therefore, the capability to build more accurate degradation models. Further these updated simulation results will help in predicting the failures and degradation in the capacitor elements with higher accuracy and precision.

## REFERENCES

- (Bengt, 1995) Alvsten Bengt. *Electrolytic Capacitors Theory and Applications*. RIFA Electrolytic Capacitors, Sweden, 1995.
- (Chen, 2004) Edward Chen. *Ripple Current Confusion*. KEME Electronic Corporation, 2004.
- (Chen, 2005) Yaow-Ming Chen. Electrolytic capacitor failure prediction of lc filter for switching-mode power converters. *Industry Applications Confer-*

- ence, 2005. *Fortieth IAS Annual Meeting*, 2(2):1464 – 1469, Oct 2005.
- (Delgado and Sira-Ramrez, 1998) Marisol Delgado and Hebertt Sira-Ramrez. A bond graph approach to the modeling and simulation of switch regulated dc-to-dc power supplies. *Simulation Practice and Theory*, page 631646, November 1998.
- (Dragan Antic and Mladenovic, 1999) Biljana Vidojkovic Dragan Antic and Miljana Mladenovic. An introduction to bond graph modelling of dynamic systems. *TELSIKS'99*, Oct 1999.
- (Fife, 2006) James Fife. Wet electrolytic capacitors. Patent No: 7,099 1, AVX Corporation, Myrtle Beach, SC, Aug 2006.
- (Garcia-Gomez *et al.*, 2006) Garcia-Gomez, S. Rimaux, and M. Delgado. Bond graphs in the design of adaptive passivity-based controllers for dc/dc power converters. *IEEE International Conference on Industrial Technology, 2006. ICIT 2006.*, pages 132–137, Dec 2006.
- (Gasperi, 1996) M. L. Gasperi. Life prediction model for aluminum electrolytic capacitors. *31st Annual Meeting of the IEEE-IAS*, 4(1):1347–1351, October 1996.
- (Gawthrop and Smith, 1996) P. J. Gawthrop and L. P. S. Smith. *Metamodelling: bond graphs and dynamic systems*. Prentice Hall, New York, NY, 1996.
- (Goodman and et al, 2005) Douglas Goodman and et al. Practical application of phm/prognostics to cots power converters. *Aerospace Conference, 2005 IEEE*, pages 3573–3578, March 2005.
- (Imam *et al.*, 2005) A.M. Imam, T.G. Habetler, R.G. Harley, and D.M. Divan. Condition monitoring of electrolytic capacitor in power electronic circuits using adaptive filter modeling. *IEEE 36th Power Electronics Specialists Conference, 2005. PESC '05.*, pages 601–607, June 2005.
- (Kalgren and et al, 2007) Patrick Kalgren and et al. Application of prognostic health management in digital electronic system. *Aerospace Conference, 2007 IEEE*, pages 1–9, March 2007.
- (Karnopp and Rosenberg, 1983) Dean Karnopp and Roland Rosenberg. *Introduction to Physical System Dynamics*. Mcgraw-Hill College, New York, NY, 1983.
- (Lahyani *et al.*, 1998) A. Lahyani, P. Venet, G. Grellet, and P.J. Viverge. Failure prediction of electrolytic capacitors during operation of a switch-mode power supply. *IEEE Transactions on Power Electronics*, 13:1199–1207, Nov 1998.
- (Luo *et al.*, 2003) Jianhui Luo, Madhavi Namburu, Krishna Pattipati, and et al. Model-based prognostic techniques. *AUTOTESTCON 2003. IEEE Systems Readiness Technology Conference. Proceedings*, pages 330– 340, Sep 2003.
- (P. Venet and Grellet, 1993) H. Darnand P. Venet and G. Grellet. Detection of faults of filter capacitors in a converter. application to predictive maintenance”, journal = ”intelec proc. 2:229–234, 1993.
- (Pecht *et al.*, 2007) Michael Pecht, B. Tuchband, N. Vichare, and Qu Jian Ying. Prognostics and health monitoring of electronics. *International Conference on Thermal, Mechanical and Multi-Physics Simulation Experiments in Microelectronics and Micro-Systems*, pages 1–8, April 2007.
- (Roychoudhury *et al.*, 2008) I. Roychoudhury, M. Daigle, G. Biswas, and X. Koutsoukos. Efficient simulation of hybrid systems: An application to electrical power distribution systems. *Proceedings of the 22nd European Conference on Modeling and Simulation*, pages 471–477, June 2008.
- (R.P.Tye, 1968) R.P.Tye. *Thermal Conductivity*. Academic Press Inc, Burlington, MA, 1968.
- (Schwabacher, 2005) Mark Schwabacher. A survey of data-driven prognostics (aiaa). *Infotech at Aerospace*, Sep 2005.
- (Vachtsevanos, 2006) George Vachtsevanos. *Intelligent Fault Diagnosis and Prognosis for Engineering Systems*. Wiley, 2006.
- (Vorperian., 1990) V. Vorperian. Simplified analysis of pwm converters using model of pwm switch.continuous conduction mode. *IEEE Transactions on Aerospace and Electronic Systems*, page 490496, May 1990.

**CHETAN KULKARNI** received the M.S. degree in EECS from Vanderbilt University, Nashville, TN, in 2009, where he is currently a Ph.D. Student. His web page is <http://people.vanderbilt.edu/chetan.kulkarni/>.

**GAUTAM BISWAS** received the Ph.D. degree in computer science from Michigan State University, East Lansing. He is a Professor of Computer Science and Computer Engineering in the Department of Electrical Engineering and Computer Science, Vanderbilt University, Nashville, TN. His web page can be found at <http://www.vuse.vanderbilt.edu/biswas/>.

**XENOFON KOUTSOUKOS** received the Ph.D. degree in electrical engineering from the University of Notre Dame, Notre Dame, IN, in 2000. He is an Assistant Professor in the Department of Electrical Engineering and Computer Science, Vanderbilt University, Nashville, TN. His web page is <http://www.vuse.vanderbilt.edu/koutsoxd/>.